Scientific Research Publishing

Open Journal of Applied Sciences, 2024, 14, 3016-3027
https://www.scirp.org/journal/ojapps
ISSN Online: 2165-3925
ISSN Print: 2165-3917

Influence of Geometric Parameters on the Radiation of a Microstrip Leaky-Wave Antenna for W-Band Applications

Charmolavy Goslavy Lionel Nkouka Moukengue, Nzonzolo, Barol Mafouna Kiminou, Désiré Lilonga-Boyenga

Laboratory of Electrical and Electronic Engineering, National Polytechnic School, Marien Ngouabi University, Brazzaville, Congo
Email: ln999kouka@gmail.com

How to cite this paper: Nkouka Moukengue, C.G.L., Nzonzolo, Kiminou, B.M. and Lilonga-Boyenga, D. (2024) Influence of Geometric Parameters on the Radiation of a Microstrip Leaky-Wave Antenna for W-Band Applications. *Open Journal of Applied Sciences*, **14**, 3016-3027.
https://doi.org/10.4236/ojapps.2024.1411198

Received: August 20, 2024
Accepted: November 4, 2024
Published: November 7, 2024

Abstract

The development of space telecommunications in recent years has necessitated the design and the realization of compact, high-performance equipment operating at increasingly high frequencies. The use of high-precision radars for surveillance, detection and mobile communication systems orients research toward the antennas to electronic sweep. In this article, we present a microstrip leaky-wave antenna with periodic patches. Its design is based on an integral formulation solved by software using HFSS finite elements. A parametric study of this antenna is validated by simulations and compared with other results found in the literature. Analysis of the antenna's radiation parameters shows that the main beam direction and levels of minor's lobes can be controlled from these geometrical parameters. The interest of this study is to meet the requirements of antennas dedicated telecommunications systems.

Keywords

Leaky-Wave Antenna, Parameters of Radiation, Software HFSS, W-Band

1. Introduction

The reduction in the size of terminals, linked to the widespread use of integrated components to the detriment of analogue elements, has made it incoherent to use conventional antennae that are too bulky, especially as the large-scale marketing of terminals has created an unprecedented demand for miniature antennae, the performance of which must take account of both the communication systems and the context of use.

Today, planar antennas are attracting a great deal of interest from researchers

because of their many uses. The main applications for microstrip antennas are in high-frequency communications, such as space communications, military systems, GPS (Global Positioning System) satellite positioning, aerial and terrestrial navigation, WLAN (Wireless Local Area Network) computer networks, and new fields, such as medicine and mobile telephony. The wide and important use of these antennas is essentially due to the various advantages they can offer over conventional antennas, such as low weight, volume and thickness, and very low manufacturing costs.

Abbas *et al*. (2011) demonstrated the effect of aspect ratio (width-to-length ratio) on the overall radiation characteristics of a rectangular microstrip patch antenna. They improved the gain of a microstrip patch antenna along with a radical variation of cross-polarized field radiation with aspect ratio obtained. They showed that the aspect ratio for which the cross-polarized field radiation is minimum for a particular patch is also presented and justified quantitatively [1].

Alsulami *et al*. (2013) have designed an antenna for single band at 2.45 GHz and dual bands at 3.3 - 3.6 and 5.0 - 6.0 GHz to support WLAN/WiMAX applications. The antenna has been designed to present omnidirectional radiation pattern. They have set up dual band antenna array placed on both top and bottom layers to obtain the desired antenna characteristics; double-sided dual-band antenna they have proposed provides omnidirectional radiation pattern with high gain [2].

The use of high-precision radars in surveillance, detection and mobile communication systems is driving research towards electronically scanned antennas [3]. Numerous electromagnetic modelling techniques have been developed in recent years to design these miniature antennas [4]-[8]. In recent years, research has focused on the study of scanning antennas, including leaky wave antennas, which are essential components in many mobile and on-board devices. Several studies have been developed with the aim of reducing levels of minor's lobes and/or controlling the direction of the main beam [3] [9]-[12].

Antenna design is now one of the most active areas of study within the field of communication studies. In contrast, applications like air traffic radar, satellite communications, and point-to-point terrestrial connection demand highly concentrated radiation patterns that also have a wideband and high gain. Because of this more focused radiation pattern, there will also be an increase in the communication range [13].

This article therefore presents a microstrip leaky-wave antenna operating in the W-band, the special feature of which is that the levels of minor's lobes, the beamwidth and the direction of the main beam can be controlled using the geometric dimensions of the antenna.

2. Numerical Model of the Leaky-Wave Antenna

In this article, we have used software for an integral formulation solved using

finite elements. Using a finite element calculation code. Finite element codes have to convert partial differential equations into a system of linear equations whose coefficients depend on the type of problem and the media; an infinite space will lead to a system of infinite dimension whose numerical resolution will not be possible.

This difficulty can be overcome by creating a problem approached by an equivalent structure in a bounded volume, with boundary conditions chosen to approximate reality as closely as possible.

For most finite element software, the most commonly used tool for electromagnetic radiation problems is simply called "radiation conditions" or "radiation surface". These conditions are expressed by the following relationship:

$$\lim_{\mathrm{IxI}\to\infty} \mathrm{IxI}^{\frac{n-1}{2}} \left(\frac{\partial}{\partial \mathrm{IxI}} - ik \right) u(x) = 0 \tag{1}$$

where x is a direction in space, k is the propagation constant in space, and $n = 3$ in our real space. As these surfaces are virtual, their placement must not affect existing electromagnetic fields.

It is recommended that these surfaces be placed in far-field zones, the calculation rule for which is given by a minimum distance d:

$$d = \frac{2D^2}{\lambda} \tag{2}$$

where D is the largest dimension of the antenna elements (Diameter in the case of a reflector antenna, for example), and λ is the wavelength.

3. Propagation and Radiation Parameters of Periodic Leaky-Waves Structures

In the case of a periodically charged structure with spatial periodicity p (Figure 1), if (Oz) is the direction of propagation of the guided wave, the configuration of the fields at a point (x, y, z) will be the same as that at the point $(x, y, z + p)$. Furthermore, Floquet's theorem [14]-[18] states that the fields at two homologous points differ by only one complex constant.

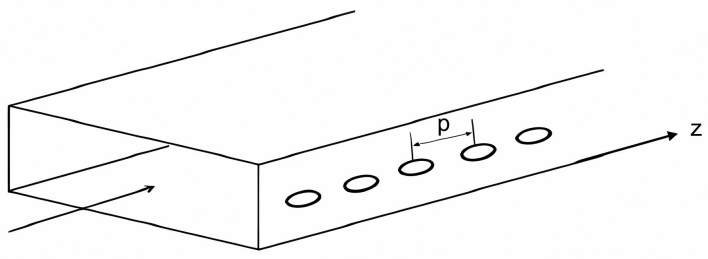

Figure 1. Periodic leaky-wave antenna.

$$E(x, y, z + d) = E(x, y, z)\mathrm{e}^{-jk_z z} \tag{3}$$

In this case, the pseudo-periodic field is decomposed into a Fourier series, giving

rise to a fundamental term ($n=0$) and space harmonics ($n=\pm1,\pm2,\cdots$) given by:

$$E(x,y,z)=\sum_{-\infty}^{+\infty}A_n(x,y)\mathrm{e}^{-jk_{zn}z} \tag{4}$$

where

$$A_n(x,y)=\frac{1}{p}\int_0^p E(x,y,z)\mathrm{e}^{+jk_{zn}z}\mathrm{d}z$$

$$k_{zn}=k_z+\frac{2\pi n}{p}=j\alpha-\left(\beta_z+\frac{2\pi n}{p}\right)$$

where $\beta_{zn}=\beta_o+\frac{2\pi n}{p}$ is the phase constant of the n^{th} harmonic; β_{zn} can take an infinity of values, β_o is the phase constant of the fundamental mode ($n=0$); α_z is the attenuation constant in z direction, $\alpha_z\sim0$, almost all values of k_{zn} are real. However, for some negative values of n, the term β_{zn} may be less than k_o , so k_{zn} is real.

The coefficient A_n of the space harmonic under consideration generally decreases with the rank n of the harmonic and the series converges rapidly so that only the fundamental term ($n=0$) is retained.

The study of periodic structures is reduced to the analysis of a single period of the structure. The total electric field is decomposed into space harmonics according to Floquet's theorem [9] [10]. We can define for each harmonic of space n, the angle corresponding to the direction of radiation. It is given by Formula (3):

$$\sin\theta_n=\frac{\beta_n}{k_o} \tag{5}$$

where $k_o=\frac{2\pi}{\lambda_o}$ is the wave number and λ_o is the length of the wave in free space. θ_n , the angle of emergence of the nth harmonic.

In practice, to avoid spurious lobes, it is advisable to work with only one fast harmonic [4]; the $n=-1$ mode is then chosen to be the radiating mode [14].

The radiation harmonic $n=-1$ in the free-espace has an angle θ_{-1} who is given by:

$$\sin\theta_{-1}=\frac{\beta_{-1}}{k_o} \tag{6}$$

where $\beta_{-z1}=\beta_{zo}-\frac{2\pi}{p}$, with p the periodicity.

4. Description

The structure studied is a microstrip leaky-wave antenna, consisting of a dielectric substrate of relative permittivity ε_r , width B, thickness a and length L_o. On the top face of the substrate, metallic patches of width w and length b were placed periodically with a period p to cause leaky-wave radiation, as shown in **Figure 2**.

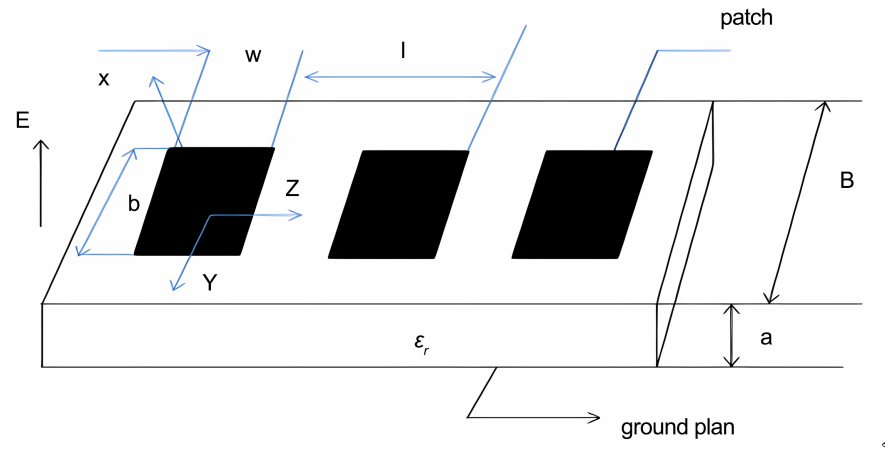

Figure 2. Microstrip leaky-wave antenna with periodic patches.

5. Pre-Determination of the Numerical Simulation Volume

For this structure, the radiation direction is normal to the dielectric substrate-metal patch-air interface. The simulation volume chosen is in the form of a box enveloping the structure to be simulated, as shown in Figure 3. The study of the simulation volume is reduced to determining the width of the dielectric substrate *B*, on which the lateral radiation surfaces depend, and the value of *H*: the thickness of the air-box above the radiating elements, which determines the upper radiation surface.

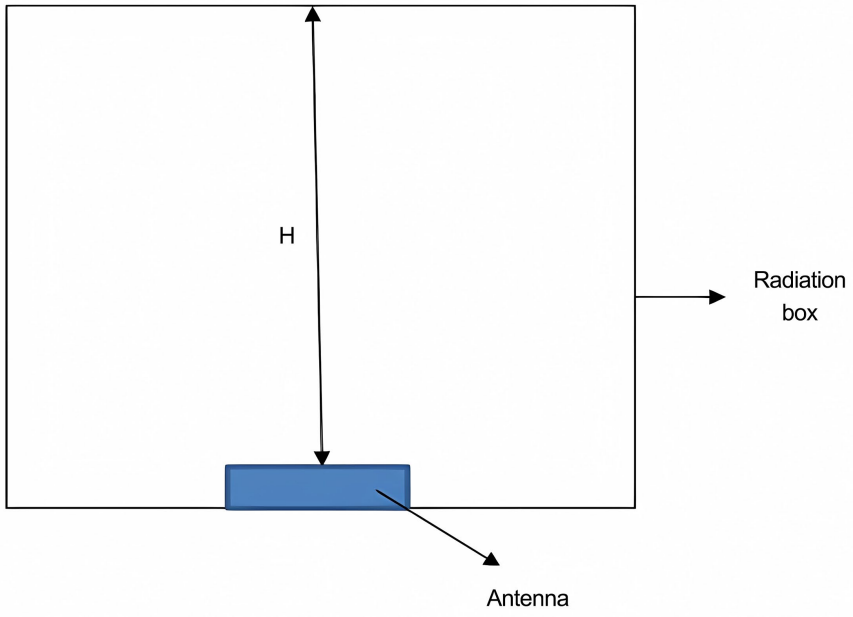

Figure 3. Radiation box of a microstrip leaky-wave antenna.

5.1. Influence of Side Walls

First, the upper radiating surface is set to a value that is large enough without over-burdening the electromagnetic simulation task: $H/\lambda_o = 8$. Different values of

distance between the radiating elements and the lateral radiating surfaces were parameterised by the choice of B/λ_o (Figure 4).

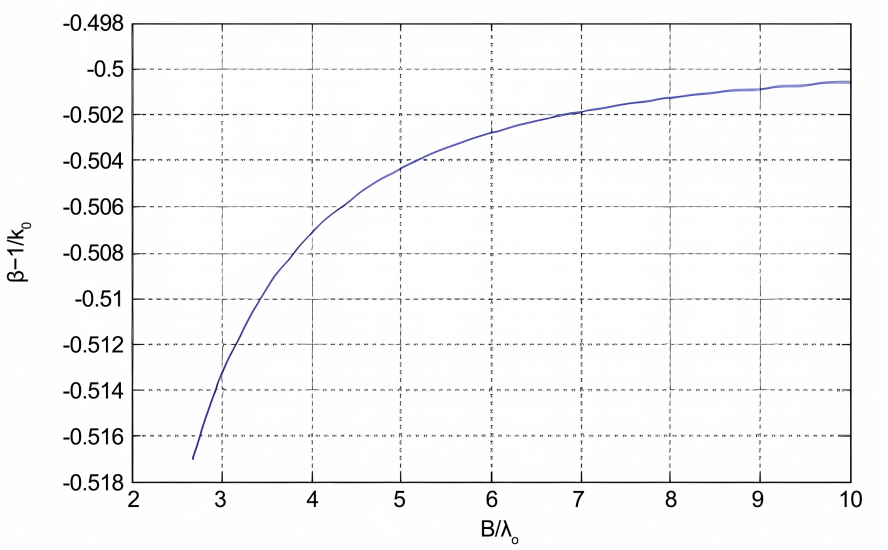

Figure 4. Variation of β_{-1}/k_0 as a function of B/λ_o at F= 80 GHz.

The first characteristic observed is the complex propagation constant, the real part of which is related to the radiation direction of the main beam. In Figure 4, the value normalised by the constant propagation in free space has been plotted as a function of the ratio B/λ_o. There is a change in the slope of the variation from a ratio of 5, meaning that the variation stabilises. Between two values, 6 and 10, the relative variation is approximately 0.02/0.5, *i.e.* 4%, for a saving in memory space of at least 30%, and a much longer calculation time.

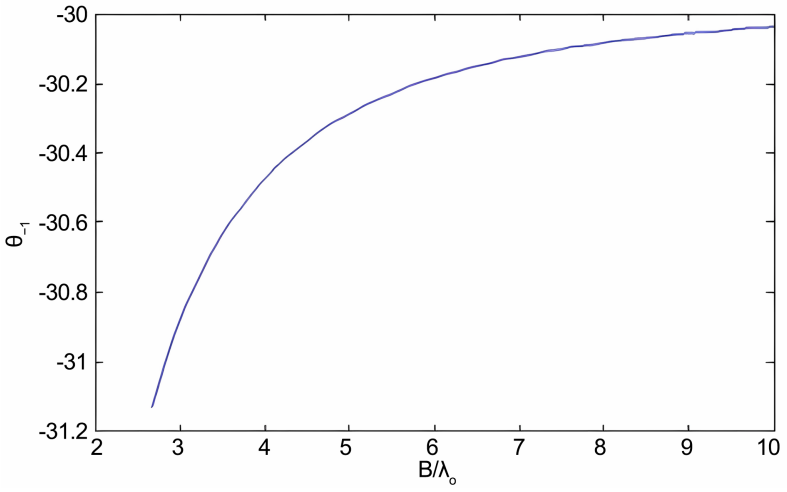

Figure 5. Main beam direction θ_{-1} as a function of B/λ_o at F= 80 GHz.

Figure 5 shows the variation in angular direction θ_{-1} as a function of B/λ_o. From a B/λ_o ratio value of 6, the variation is Sensibly negligible.

From the point of view of finding the complex propagation constant, a B/λ_o ratio of between 7 and 10 is an acceptable compromise.

5.2. Influence of the Upper Radiation Surface

The study of positioning of the upper radiation surface was carried out by fixing the substrate width in the region of values between 7 and 10 times the wavelength, and with several values of the air box height. Results on the radiation pattern are given in **Figure 6**, and compared with those published by Ghomi in [3], who used the transverse resonance method.

If the difference between the reference and the choice of a low air height is significant, the addition of a layer of air of 2.6 to 3 wavelengths enables the results of Ghomi [3] to be approached.

Given the results obtained, an air box height of between 8 and 10 times the wavelength seems sufficient to obtain acceptable results. However, it is advisable to take into account the complexity of the antennae and the computer resources available on the workstation, in particular, the amount of RAM, which determines the choice of algorithm for solving the final linear system.

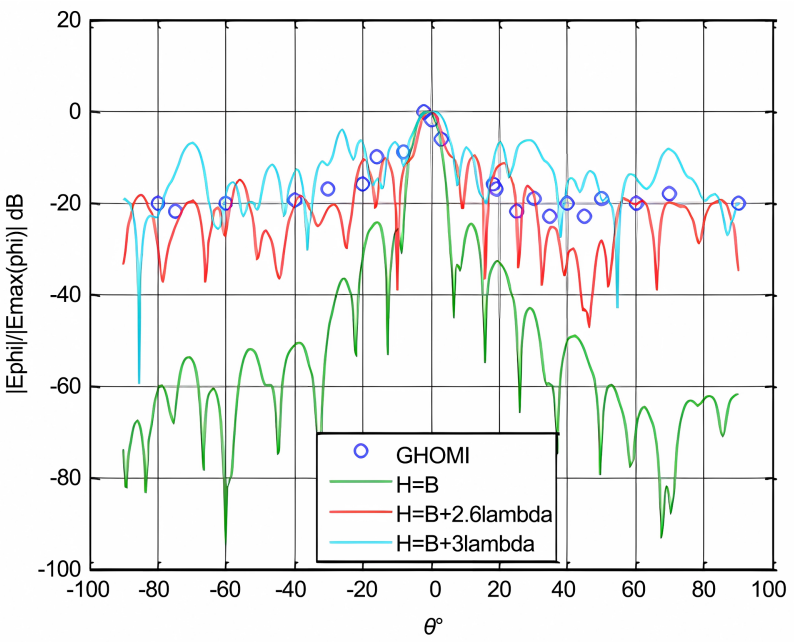

Figure 6. Radiation pattern of the E-plane leaky wave antenna at $F = 80$ GHz.

6. Results and Discussion

This section presents the simulation results of the proposed Microstrip Leaky Wave Antenna. The system was designed and simulated using the High Frequency Structure Simulation software (HFSSv13).

6.1. Radiation Parameters

In **Figure 7** and **Figure 8**, a comparison between these radiation patterns is made

with those obtained by [1] using the Transverse Resonance Method (TRM) for 11 and 25 patch elements at 80 GHz. The curves found with the HFSS software and the experimental diagrams obtained by the reference merge, particularly in the vicinity of the main beam over an angular aperture of 6˚. A remarkable asymmetry in the position of two sidelobes on either side of the sidelobes is observed.

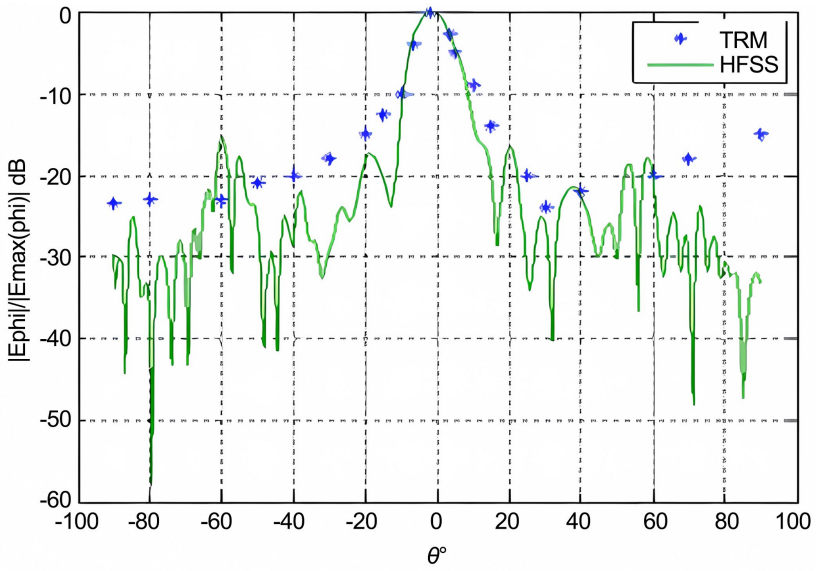

Figure 7. Radiation pattern in the E-plane at $F = 80$ GHz, $b = 0.8\lambda_o$, $N = 25$, $\varepsilon_r = 2.46$, $w = 0.3387\lambda_o$, $B = 8\lambda_o$.

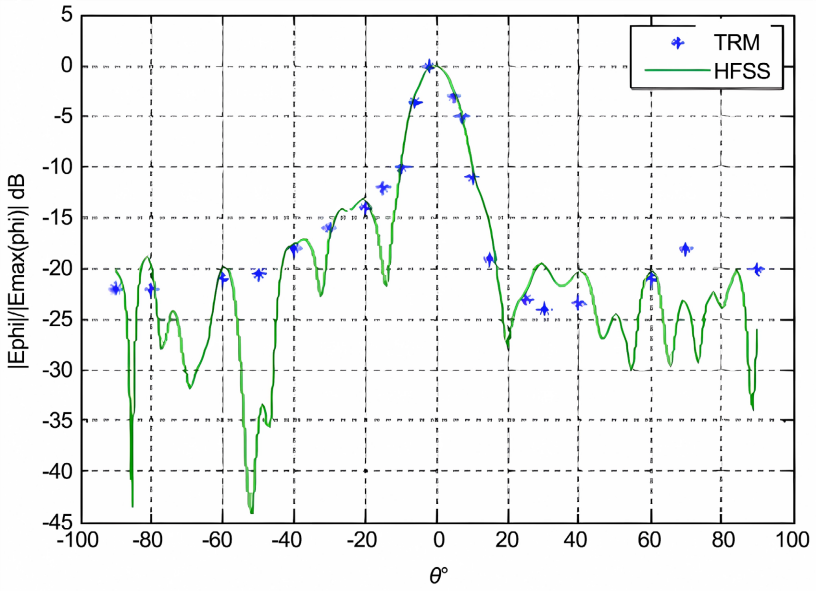

Figure 8. Radiation pattern in the E-plane at $F = 80$ GHz, $b = 0.8\lambda_o$, $N = 11$, $\varepsilon_r = 2.46$, $w = 0.3387\lambda_o$, $B = 8\lambda_o$.

We can see that the levels of minor's lobes depend directly on the number of metal patches, as shown in **Figure 9**. As this number increases, the levels of minor's

lobes decrease. A remarkable asymmetry in the position of two sidelobes on either side of the main lobe is observed.

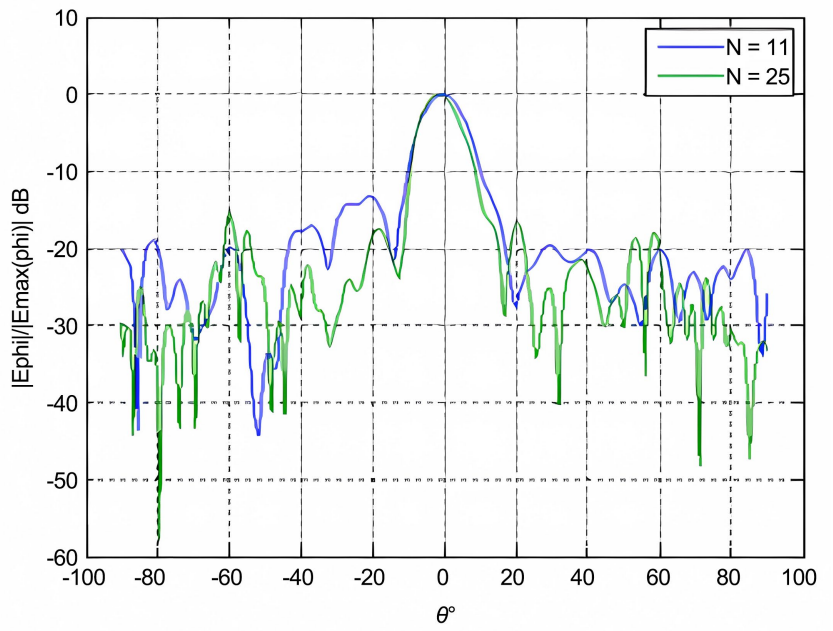

Figure 9. Radiation pattern in the E-plane at $F = 80$ GHz, $b = 0.8\lambda_o$, $\varepsilon_r = 2.46$, $w = 0.3387\lambda_o$, $B = 8\lambda_o$.

6.2. Influence of Geometric Dimensions

Figure 10 and **Figure 11** show the radiation diagrams, taking into account variations in the width of the dielectric substrate and the geometric dimensions of the patches.

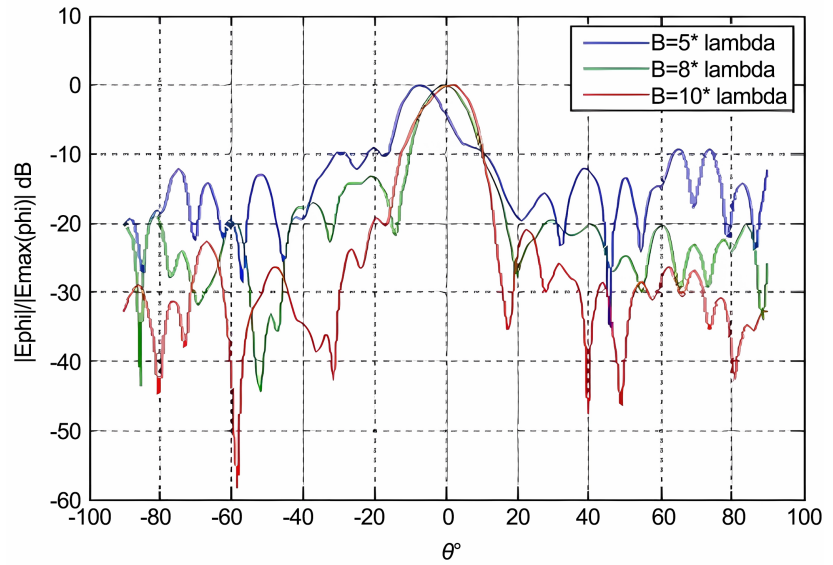

Figure 10. Radiation pattern of the E-plane leaky wave antenna ($\varphi = 90^\circ$), $F = 80$ GHz, $w = 0.3387\lambda_o$, $N = 11$.

In Figure 10, the radiation pattern has been simulated taking into account the width of the dielectric substrate. The purpose of increasing the latter is to make this pattern more directional with a low level of minor's lobes and the position of the beam direction is −8.7˚, −3˚ and 1˚ for $B = 5\lambda_o$, $B = 8\lambda_o$ and $B = 11\lambda_o$, respectively. We note that the bandwidth increases as the substrate width decreases.

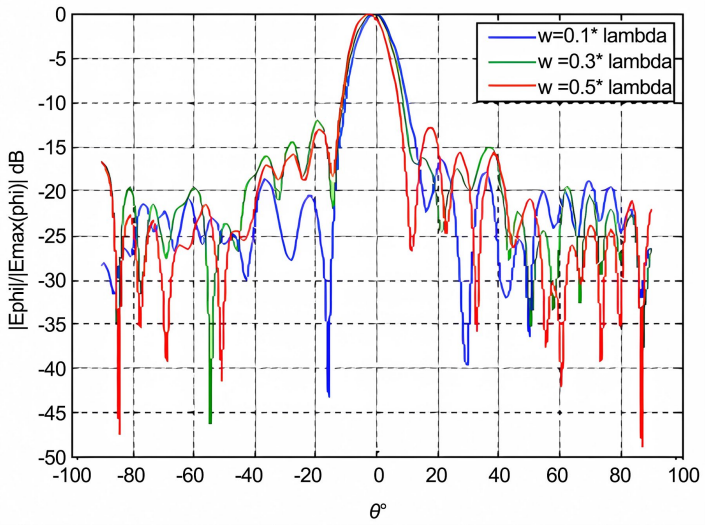

Figure 11. Radiation pattern of the E-plane leaky wave antenna, $b = 0.8\lambda_o$, $F = 80$ GHz, $N = 11$, $\varepsilon_r = 2.46$.

Figure 11 shows the radiation pattern of an LWA, varying the width of the patch. There is a clear shift of the main beam to the right for decreasing values of *w*. The position of angular depointing is almost constant for values of w less than or equal to $0.3387\lambda_o$.

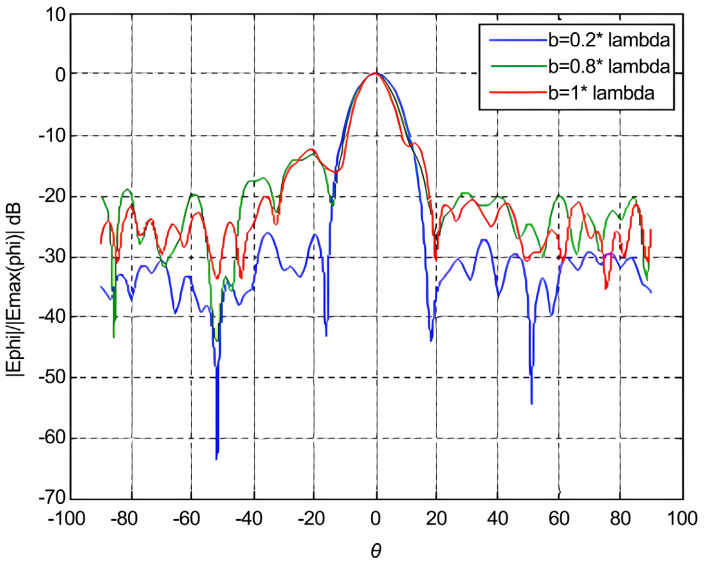

Figure 12. Radiation pattern of the E-plane leaky wave antenna, $F = 80$ GHz, $N = 11$, $w = 0.332\lambda_o$, $\varepsilon_r = 2.46$.

In Figure 12, the radiation pattern is shown for different values of patch length *b*. The angular depointing is almost constant, as can be seen, but an increase in the levels of minor's lobes is visible as *b* increases.

7. Conclusion

In this article, a microstrip leaky-wave antenna with periodic patches has been proposed. Simulation results have shown that the angular depointing and levels of minor's lobes can be controlled by varying the width of the dielectric substrate or the geometric dimensions of the patches. This antenna can be applied in Radar systems.

Conflicts of Interest

The authors declare no conflicts of interest regarding the publication of this paper.

References

[1] Abbas, S.Md.D., Paul, S., Sen, J., Gupta, P.R., Malakar, K., Chattopadhyay, S., *et al.* (2011) Aspect Ratio: A Major Controlling Factor of Radiation Characteristics of Microstrip Antenna. *Journal of Electromagnetic Analysis and Applications*, **3**, 452-457. https://doi.org/10.4236/jemaa.2011.311072

[2] Alsulami, R. and Song, H. (2013) Double-Sided Microstrip Circular Antenna Array for WLAN/WiMAX Applications. *Journal of Electromagnetic Analysis and Applications*, **5**, 182-188. https://doi.org/10.4236/jemaa.2013.54029

[3] Ghomy, M. (1992) Contribution à l'étude des antennes micro-rubans à ondes de fuite. Thèse de Doctorat, INP-Toulouse.

[4] Liu, J., Tang, X., Li, Y. and Long, Y. (2012) Substrate Integrated Waveguide Leaky-Wave Antenna with H-Shaped Slots. *IEEE Transactions on Antennas and Propagation*, **60**, 3962-3967. https://doi.org/10.1109/tap.2012.2201085

[5] Doucha, S., Abri, M., *et al.* (2015) Leaky Wave Antenna Design Based on SIW Technology for Millimeter Wave Applications. *WSEAS Transactions on Communications*, **14**, 108-112.

[6] Mohammad-Ali-Nezhad, S. and Mallahzadeh, A. (2015) Periodic Ridged Leaky-Wave Antenna Design Based on SIW Technology. *IEEE Antennas and Wireless Propagation Letters*, **14**, 354-357. https://doi.org/10.1109/lawp.2014.2361175

[7] Razafimahatratra, S., Mavridis, T., *et al.* (2015) Antenne cornet SIW pour réseaux de capteurs corporels à 60 GHz. *XIXèmes Journées Nationales Microondes*, Bordeaux, 3-5 Juin 2015, 1-5.

[8] Moukengue, N., *et al.* (2019) A 80 GHz Microstrip Leaky-Wave Antenna with De-graded Ground Plane Design. *Journal of Scientific and Engineering Research*, **6**, 97-101.

[9] El Hal, G., Souleau, R., *et al.* (2011) Antenne à ondes de fuite à balayage angulaire à fréquence fixe à 77 GHz. 17*é Journée Nationale Micro-Ondes*, Brest, 18-20 Mai 2011, 1-4.

[10] Shahvarpour, A., *et al.* (2010) Anisotropic Meta-Substrate Conical-Beam Leaky-Wave Antenna. *Proceedings of Asia-Pacific Microwave Conference*, Yokohama, 7-10 December 2010, 299-302.

[11] Charmolavy, G.L., Moukengue, N. and Mafouna Kiminou, B. (2023) Effect of Coupling on the Performance a Periodic Leaky Wave Patch Antenna. *International Journal of*

Engineering & Technology, **12**, 1-6. https://doi.org/10.14419/ijet.v12i1.32289

[12] Charmolavy, G.L., Moukengue, N. and Gogom, R. (2023) Influence of Patchs Shape on the Radiation Performance a Microstrip Leaky-Wave Antenna. *International Journal of Engineering Technology and Management Sciences*, **7**, 449-454. https://doi.org/10.46647/ijetms.2023.v07i05.055

[13] Jennie Bharathi, R. and Neduncheliyan, S. (2023) Wideband SIW Based Slot Antenna for RADAR Applications. *Journal of Physics*: *Conference Series*, **2484**, Article ID: 012054. https://doi.org/10.1088/1742-6596/2484/1/012054

[14] Collin, R.E. (1991) Theory of Guides Waves. 2nd Edition, OEEE Press.

[15] Lilonga-Boyenga, D. (1984) Contribution à l'étude du couplage par onde de charge d'espace dans les structures interdigitale et bigrille. Thèse de Doctorat, INP-Toulouse.

[16] Trinh, T.N., Mittra, R. and Paleta, R.J. (1981) Horn Image-Guide Leaky-Wave Antenna. *IEEE Transactions on Microwave Theory and Techniques*, **29**, 1310-1314. https://doi.org/10.1109/tmtt.1981.1130557

[17] Schwering, F. and Oliner, A.A. (1988) Millimeter-Wave Antennas. In: Lo, Y.T. and Lee, S.W., Eds., *Antenna Handbook*, Springer US, 1135-1282. https://doi.org/10.1007/978-1-4615-6459-1_17

[18] Honey, R. (1959) A Flush-Mounted Leaky-Wave Antenna with Predictable Patterns. *IRE Transactions on Antennas and Propagation*, **7**, 320-329. https://doi.org/10.1109/tap.1959.1144703